

# Certifying Stability and Performance of Uncertain Differential-Algebraic Systems: A Dissipativity Framework

Emily Jensen, *Member, IEEE*, Neelay Junnarkar, *Student Member, IEEE*, Murat Arcak, *Fellow, IEEE*, Xiaofan Wu, Suat Gumussoy, *Senior Members, IEEE*

**Abstract**—This paper presents a novel framework for characterizing dissipativity of uncertain systems whose dynamics evolve according to differential-algebraic equations. Sufficient conditions for dissipativity (specializing to, e.g., stability or  $L_2$  gain bounds) are provided in the case that uncertainties are characterized by integral quadratic constraints. For polynomial or linear dynamics, these conditions can be efficiently verified through sum-of-squares or semidefinite programming. Performance analysis of the IEEE 39-bus power network with a set of potential line failures modeled as an uncertainty set provides an illustrative example that highlights the computational tractability of this approach; conservatism introduced in this example is shown to be quite minimal.

## I. INTRODUCTION

Dissipativity theory [1] relates input-output properties of dynamical systems to the dissipation of so-called *storage functions* over trajectories [2]. Storage functions generalize Lyapunov functions to systems with inputs and outputs: the time derivative of the storage function along trajectories is upper bounded by a *supply rate* that describes a relation of the system’s inputs and outputs. Appropriate

This work was supported in part by Siemens Corporation R&D funding and by the NSF grant CNS-2135791.

Emily Jensen, Neelay Junnarkar, and Murat Arcak are with the department of Electrical Engineering and Computer Sciences at the University of California, Berkeley. (emails: {emilyjensen, neelay.junnarkar, arcak}@berkeley.edu)

Xiaofan Wu and Suat Gumussoy are with Siemens Technology. (emails: {xiaofan.wu, suat.gumussoy}@siemens.com)

choices of supply rate lead to important cases of dissipativity, such as passivity and stability, as well as  $L_2$  gain bounds ( $H_\infty$  norm) which is key to robustness analysis. Moreover, a dissipativity framework allows for incorporation of uncertainties described by integral quadratic constraints (IQCs) [3], [4]. This will be key to developing our main result, which provides a sufficient condition for dissipativity of uncertain systems described by differential algebraic equations (DAEs).

Classical dissipativity applies to system dynamics described by ordinary differential equations (ODEs), and sufficient conditions for dissipativity of uncertain ODE systems have been developed [5]. Despite the vast literature on dissipativity and on DAEs, a general dissipativity framework for uncertain and nonlinear differential-algebraic systems is lacking, and this work addresses this gap.

DAEs model dynamical systems with inherent algebraic constraints and arise in chemical, electrical, and mechanical engineering applications [6], e.g., the inherent conservation of charge can be modeled as a constraint in electric circuit dynamics, incompressibility can be captured as a constraint in fluid flow modeled by the Navier-Stokes equations, or holonomic constraints can be used to model mechanical system motion [7]. Many classical results have been extended from the ODE to the DAE setting, including controllability and observability [8], and controller [9] and observer [10] design for linear systems. Specific subclasses of dissipativity that have been examined for DAEs include positive

realness of linear DAE systems [11] and Lyapunov stability and passivity of nonlinear DAE systems [12]. However, incorporation of uncertainties into dissipativity analysis of DAE systems is less prevalent, and this work addresses this gap. One exception is [13] which analyzes stability of linear DAE systems subject to polytopic uncertainties.

This work is motivated by DAE models with algebraic constraints that model underlying network interconnections, e.g., dynamics of multibody systems with interconnection constraints [14], power networks with algebraic constraints describing the power flow equations [15], and implicit neural networks with outputs defined as the solutions to fixed-point equations [16]. When the algebraic constraint is invertible, the DAE system may be equivalently represented as a standard ODE, e.g., power network DAEs can be converted to an ODE through a Kron reduction procedure [17]. However, when the algebraic constraint captures underlying graph properties, it may be desirable to preserve this form to incorporate uncertainties or changes to the graph in a way that preserves the graph structure. In other cases, the algebraic conditions may not be invertible or an inversion may be ill-conditioned or computationally challenging.

In this manuscript, we provide *sufficient conditions for dissipativity of DAE systems with uncertainties described by quadratic constraints*. For linear or polynomial dynamics, we show that *these conditions can be verified numerically with linear matrix inequalities or Sum-of-Squares programming*, respectively. Throughout, we emphasize computational tractability of the conditions derived, at the expense of some conservatism. We illustrate the usefulness of this choice in Section V, where the performance of a power network subject to an uncertain line failure is quickly verified.

The remainder of the paper is structured as follows. In Section II, the DAE model of interest with uncertainties characterized by IQCs is presented; the notion of dissipativity for this model is formalized. Section III presents a sufficient condition for dissipativity of uncertain DAE systems. Numerical methods to confirm this condition are noted in Section III-A and Section IV for polynomial and linear

dynamics, respectively. A power network with an uncertain line failure is analyzed as a case study in Section V.

## II. PROBLEM SET-UP: UNCERTAIN DIFFERENTIAL-ALGEBRAIC SYSTEMS

We consider a time-invariant system with state dynamics described by an ordinary-differential equation along with an algebraic condition:

$$\dot{\mathbf{x}}(t) = f(\mathbf{x}(t), \mathbf{v}(t), \mathbf{w}(t), \boldsymbol{\xi}(t)) \quad (1a)$$

$$0 = g(\mathbf{x}(t), \mathbf{v}(t), \mathbf{w}(t), \boldsymbol{\xi}(t)) \quad (1b)$$

$$\mathbf{y}(t) = h(\mathbf{x}(t), \mathbf{v}(t)), \quad (1c)$$

where  $\mathbf{x}(t) \in \mathbb{R}^n$  is the state,  $\mathbf{v}(t) \in \mathbb{R}^m$  is the algebraic variable,  $\mathbf{w}(t) \in \mathbb{R}^p$  is an exogenous disturbance with finite energy ( $\|\mathbf{w}\|_{L_2} < \infty$ ), and  $\mathbf{y}(t) \in \mathbb{R}^q$  is an output.  $\boldsymbol{\xi}(t) \in \mathbb{R}^\ell$  captures additional dynamics, e.g., uncertainties, and is modeled as the output of a bounded, causal system  $\Delta : L_2^n \times L_2^m \rightarrow L_2^\ell$ :

$$\boldsymbol{\xi} = \Delta(\mathbf{x}, \mathbf{v}). \quad (2)$$

Bold letters denote signals,  $\mathbf{x} : [0, \tau] \rightarrow \mathbb{R}^n$ , and non-bold letters denote points,  $x \in \mathbb{R}^n$ . We assume an equilibrium point exists and is shifted to  $x = 0$ ; i.e.,  $f(0, v_0, 0, 0) = 0, g(0, v_0, 0, 0) = 0$  for some  $v_0$ . For  $\boldsymbol{\xi} = 0$ , (1) is a *differential-algebraic equation* (DAE) in *semi-explicit form* [7], [6].

*Assumption 1:* The initial conditions of (1) are *consistent*, e.g., they satisfy the algebraic condition (1b). Inputs to the system are sufficiently smooth<sup>1</sup>.

Under Assumption 1, a unique solution  $\mathbf{x}, \mathbf{v}, \boldsymbol{\xi}, \mathbf{y}$ , exists for system (1)-(2) over an interval of time  $t \in [0, \tau]$ . Methods for determining admissible initial conditions can be found in, e.g., [18], and existence and uniqueness of solutions can be confirmed through, e.g., geometric approaches [19], [20], theory of differential equations on manifolds [21], or computational methods [22]. Further details are beyond the scope of this work; we refer the reader to [7], [6] and the references therein for a more comprehensive study.

<sup>1</sup>When  $\frac{\partial g}{\partial \mathbf{v}}$  is nonsingular, the DAE is of *index 1* [7]; for higher index systems, the solution of (1) will be dependent on derivatives of the input  $w$  [6].

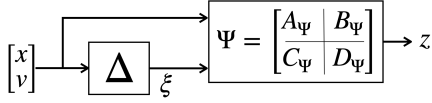


Fig. 1. Block diagram representation of uncertain system  $\Delta$  and virtual filter  $\Psi$ .  $\Psi$  is utilized to provide a more general input-output characterization of  $\Delta$  via the integral quadratic constraint  $\int_0^\infty z(t)^\top M z(t) dt \leq 0$  for some  $M = M^\top$ , where  $z$  is the output of  $\Psi$ .

### A. Dissipativity of DAE Systems

We begin by formalizing the notion of dissipativity for uncertain DAE systems.

*Definition 1:* Under Assumption 1, the DAE system (1)-(2) is *dissipative* with respect to the supply rate  $s(\cdot, \cdot)$  if there exists a *storage function*  $V$ , that is positive and satisfies  $V(0) = 0$  and

$$V(\mathbf{x}(T)) - V(\mathbf{x}(0)) \leq \int_0^T s(\mathbf{w}(t), h(\mathbf{x}(t), \mathbf{v}(t))) dt \quad (3)$$

for all  $T \in [0, \tau]$ .

Note that  $\mathbf{x}, \mathbf{w}, \mathbf{v}$ , and  $\xi$  in (3) satisfy the dynamics (1). Supply rates of interest include:

- $s(w, y) = w^\top y$  corresponding to *passivity*,
- $s(w, y) = w^\top w - \gamma^2 y^\top y$  corresponding to an  $L_2$  *gain bound* of  $\gamma$ ,
- $s(w, y) \equiv 0$  corresponding to *stability* of the origin; in this case, the storage function  $V(\cdot)$  serves as a Lyapunov function.

As with the standard ODE setting, this definition is difficult to verify in uncertain settings, i.e., with presence of unknown  $\Delta$ . In what follows, we derive sufficient conditions for dissipativity when  $\Delta$  is unknown, but satisfies known quadratic constraints.

### B. Integral Quadratic Constraints

Incorporation of uncertainties is a key component of our framework, which will develop sufficient conditions for dissipativity of *uncertain* DAE systems. Toward this aim, we utilize an integral quadratic constraint framework, which has previously been incorporated into dissipativity analysis in the ODE setting [3].

We characterize  $\Delta$  in (2) through input-output properties with the framework of integral quadratic constraints (IQCs) [4], [23]. As depicted in Figure 1, the input signals  $\mathbf{x}, \mathbf{v}$  and output signal  $\xi$

of  $\Delta$  are passed through a “virtual filter”  $\Psi$  defined by the stable linear dynamics:

$$\begin{aligned} \dot{\psi}(t) &= A_\Psi \psi(t) + B_\Psi \begin{bmatrix} \mathbf{x}(t) \\ \mathbf{v}(t) \\ \xi(t) \end{bmatrix}, \quad \psi(0) = 0 \\ z(t) &= C_\Psi \psi(t) + D_\Psi \begin{bmatrix} \mathbf{x}(t) \\ \mathbf{v}(t) \\ \xi(t) \end{bmatrix}. \end{aligned} \quad (4)$$

For  $M = M^\top$ ,  $\Delta$  satisfies the *hard IQC* defined by  $(\Psi, M)$  if

$$\int_0^T z(t)^\top M z(t) dt \leq 0 \quad (5)$$

for all  $T \geq 0$ . This is clearly satisfied if

$$z(t)^\top M z(t) \leq 0, \quad \forall t \geq 0, \quad (6)$$

and we say  $\Delta$  satisfies the *pointwise quadratic constraint* defined by  $(\Psi, M)$ . In the simple case that  $\Psi$  is the identity operator, (5) reduces to

$$\int_0^T \begin{bmatrix} \mathbf{x}(t) \\ \mathbf{v}(t) \\ \xi(t) \end{bmatrix}^\top M \begin{bmatrix} \mathbf{x}(t) \\ \mathbf{v}(t) \\ \xi(t) \end{bmatrix} dt \leq 0. \quad (7)$$

## III. CONDITIONS FOR DISSIPATIVITY OF DIFFERENTIAL-ALGEBRAIC SYSTEMS

This section presents a sufficient condition for dissipativity of DAE systems with uncertainties described by IQCs; a method for confirming this condition numerically in the case of polynomial DAEs is illustrated.

*Theorem 1:* Consider the DAE system (1)-(2) and assume  $\Delta$  satisfies the IQC defined by  $(\Psi, M)$ . This system is dissipative w.r.t. the supply rate  $s(\cdot, \cdot)$  if there exist  $\tau, \lambda \geq 0$ , a matrix  $P_\Delta \succeq 0$ , and a positive definite  $V(\cdot)$  satisfying  $V(0) = 0$  and

$$\begin{aligned} &\nabla V(\mathbf{x})^\top f(\mathbf{x}, \mathbf{v}, \mathbf{w}, \xi) + \psi^\top P_\Delta \left( A_\Psi \psi + B_\Psi \begin{bmatrix} \mathbf{x} \\ \mathbf{v} \\ \xi \end{bmatrix} \right) \\ &+ \left( A_\Psi \psi + B_\Psi \begin{bmatrix} \mathbf{x} \\ \mathbf{v} \\ \xi \end{bmatrix} \right)^\top P_\Delta \psi \\ &\leq s(\mathbf{w}, h(\mathbf{x}, \mathbf{v})) + \lambda g(\mathbf{x}, \mathbf{v}, \mathbf{w}, \xi)^\top g(\mathbf{x}, \mathbf{v}, \mathbf{w}, \xi) + \\ &\tau \left( C_\Psi \psi + D_\Psi \begin{bmatrix} \mathbf{x} \\ \mathbf{v} \\ \xi \end{bmatrix} \right)^\top M \left( C_\Psi \psi + D_\Psi \begin{bmatrix} \mathbf{x} \\ \mathbf{v} \\ \xi \end{bmatrix} \right), \end{aligned} \quad (8)$$

for all  $\psi, x, v, \xi, w$ .

The left hand side of inequality (8) is the derivative of a storage function

$$\tilde{V}(x, \psi) := V(x) + \psi^\top P_\Delta \psi \quad (9)$$

for the augmented system of DAE (1) and filter (4). The terms on the right hand side of the inequality following the supply rate arise from the algebraic constraint (1b) and the incorporation of uncertainty. When uncertainty is characterized by a *pointwise* constraint, we may assume  $P_\Delta = 0$ . Nonzero  $P_\Delta$  introduces an additional term to the left hand side of (8) whose negativity may help this inequality hold.

*Proof of Theorem 1:* Integrating (8) from  $t = 0$  to  $T$  along trajectories of (1) and (4) and using the filter initial condition  $\psi(0) = 0$  gives

$$\begin{aligned} & V(\mathbf{x}(T)) + \psi(T)^\top P_\Delta \psi(T) - V(\mathbf{x}(0)) \\ & - \int_0^T s(\mathbf{w}(t), h(\mathbf{x}(t), \mathbf{v}(t))) dt \\ & \leq \lambda \int_0^T (\star)^\top g(\mathbf{x}(t), \mathbf{v}(t), \mathbf{w}(t), \boldsymbol{\xi}(t)) dt + \\ & \tau \int_0^T (\star)^\top M \left( C_\psi \psi(t) + D_\psi \begin{bmatrix} \mathbf{x}(t) \\ \mathbf{v}(t) \\ \boldsymbol{\xi}(t) \end{bmatrix} \right) dt, \end{aligned} \quad (10)$$

where terms denoted by  $(\star)$  can be inferred by symmetry. Non-positivity of the terms on the right hand side of (10) follow from (1b) and that  $\Delta$  satisfies the IQC defined by  $(\Psi, M)$ . By the classical S-procedure, non-positivity of these terms imply

$$\begin{aligned} & V(\mathbf{x}(T)) - V(\mathbf{x}(0)) + \psi(T)^\top P_\Delta \psi(T) \leq \\ & \int_0^T s(\mathbf{w}(t), h(\mathbf{x}(t), \mathbf{v}(t))) dt. \end{aligned} \quad (11)$$

(3) follows from (11) since  $P_\Delta \succeq 0$ . ■

A source of conservatism for Theorem 1 arises from requiring a *single* storage function  $\tilde{V}(\cdot, \cdot)$  to ensure dissipativity *for all*  $\Delta$  satisfying a quadratic constraint. This conservatism allows us to avoid the computational burden associated with finding a separate storage function for each separate  $\Delta$  satisfying the IQC. Additional conservatism arises because the S-procedure applied is, in general, not lossless.

Note that the condition (8) for dissipativity simplifies in the case of no uncertainty to:

$$\begin{aligned} & \nabla V(x)^\top f(x, v, w, 0) \leq \\ & s(w, h(x, v)) + \lambda g(x, v, w, 0)^\top g(x, v, w, 0). \end{aligned} \quad (12)$$

Theorem 1 is related to the stability analysis of linear DAE systems with polytopic uncertainties presented in [13]. Theorem 1 extends this notion to more general notions of dissipativity and allows for nonlinear dynamics.

#### A. Numerical Solutions for Polynomial Dynamics

When the DAE system is described by polynomials, the storage function (9) can be found numerically with a sum-of-squares approach.

A polynomial  $p$  is *sum-of-squares* (SOS) if there exist polynomials  $p_1, \dots, p_n$  such that  $p = \sum_{i=1}^n p_i^2$ . A polynomial being SOS implies it is nonnegative. Let  $\Sigma[x]$  be the set of SOS polynomials in  $x$ , and  $\Sigma[(x, v, w, \xi, \psi)]$  be the set of SOS polynomials in  $x, v, w, \xi$  and  $\psi$ . Then, for polynomial  $f, g$ , and  $h$  and a polynomial supply rate  $s$ , we can verify dissipativity through Theorem 1 by finding nonnegative scalars  $\tau$  and  $\lambda$ , a positive definite matrix  $P_\Delta$ , and a  $V \in \Sigma[x]$  such that  $V(x) - \epsilon x^\top x \in \Sigma[x]$  and

$$\begin{aligned} & s(w, h(x, v)) + \lambda \cdot (\star)^\top g(x, v, w, \xi) \\ & + \tau \cdot (\star)^\top M \left( C_\psi \psi + D_\psi \begin{bmatrix} x \\ v \\ \xi \end{bmatrix} \right) \\ & - \nabla V(x)^\top f(x, v, w, \xi) - \psi^\top P_\Delta \psi \\ & - \psi^\top P_\Delta \left( A_\psi \psi + B_\psi \begin{bmatrix} x \\ v \\ \xi \end{bmatrix} \right) \\ & \in \Sigma[(x, v, w, \xi, \psi)] \end{aligned} \quad (13)$$

where  $\epsilon$  is small and positive and each of the terms  $(\star)$  can be inferred by symmetry.

*Example 1:* Consider the polynomial DAE system:

$$\begin{aligned} \dot{\mathbf{x}}_1(t) &= -\mathbf{x}_1(t) + \mathbf{v}(t) \\ \dot{\mathbf{x}}_2(t) &= -\mathbf{x}_1(t) - \mathbf{x}_2(t) \\ 0 &= \mathbf{x}_1(t)^2 + (\mathbf{x}_2(t)^2 + 5) \mathbf{v}(t). \end{aligned} \quad (14)$$

Applying (13) to this system to show stability of the origin gives the following equations

$$\begin{aligned} V(x) - \epsilon x^\top x &\in \Sigma[x], \\ \lambda g(x, v)^\top g(x, v) - \nabla V(x)^\top f(x, v) &\in \Sigma[(x, v)]. \end{aligned}$$

To implement this, we use the SOSTOOLS MATLAB toolbox [24] and the SeDuMi solver [25]. We allow  $V$  to be a polynomial of degree  $\leq 4$ . For  $\epsilon = 10^{-3}$ , SeDuMi finds a solution  $\lambda = 0.59504$  and  $V(x) = 0.00017634x_1^4 + 0.0012261x_1^2x_2^2 + 0.0027498x_1x_2^3 + 0.0023039x_2^4 + 0.013246x_1^3 - 0.013733x_1^2x_2 - 0.055089x_1x_2^2 - 0.056305x_2^3 + 0.40316x_1^2 + 0.67688x_1x_2 + 0.57717x_2^2$ .

#### IV. DISSIPATIVITY OF LINEAR DIFFERENTIAL-ALGEBRAIC SYSTEMS

For linear DAE dynamics, dissipativity can be verified with feasibility of an LMI. The linear DAE model is:

$$\dot{\mathbf{x}}(t) = \mathbf{A}\mathbf{x}(t) + \mathbf{B}_v\mathbf{v}(t) + \mathbf{B}_w\mathbf{w}(t) + \mathbf{B}_\xi\xi(t) \quad (15a)$$

$$0 = \mathbf{F}\mathbf{x}(t) + \mathbf{G}_v\mathbf{v}(t) + \mathbf{G}_w\mathbf{w}(t) + \mathbf{G}_\xi\xi(t) \quad (15b)$$

$$\mathbf{y}(t) = \mathbf{C}\mathbf{x}(t) + \mathbf{D}_v\mathbf{v}(t), \quad (15c)$$

where

$$\xi = \Delta(\mathbf{x}, \mathbf{v}) \quad (16)$$

can describe nonlinearities such as model uncertainties [26] or saturations [27]. We restrict our attention to *quadratic* supply rates:

$$s(w, y) = \begin{bmatrix} y \\ w \end{bmatrix}^\top \tilde{X}_s \begin{bmatrix} y \\ w \end{bmatrix}$$

which, using the equality  $y = \mathbf{C}\mathbf{x} + \mathbf{D}_v\mathbf{v}$ , can be written as

$$s(w, \mathbf{C}\mathbf{x} + \mathbf{D}_v\mathbf{v}) = \begin{bmatrix} \mathbf{x} \\ \mathbf{w} \end{bmatrix}^\top \begin{bmatrix} X_{xx} & X_{xw} \\ X_{xw}^\top & X_{ww} \end{bmatrix} \begin{bmatrix} \mathbf{x} \\ \mathbf{w} \end{bmatrix} \quad (17)$$

For linear dynamics and quadratic supply rates, there is no loss [1] in restricting a storage function  $V(\cdot)$  to be quadratic:

$$V(x) = x^\top Px, \quad P = P^\top \succ 0. \quad (18)$$

The proof of the following result is presented in Appendix B.

*Proposition 1:* Consider the linear DAE system (15)-(16) with  $\Delta$  satisfying the IQC defined by  $(\Psi, M)$ . This system is dissipative w.r.t. the

quadratic supply rate (17) if there exists  $\lambda, \tau \geq 0$ ,  $P \succ 0$ , and  $P_\Delta \succeq 0$  satisfying

$$\begin{aligned} &\left[ \begin{array}{cc|c} X(P) & PB_w & B_\psi^\top P_\Delta \\ B_w^\top P & 0 & 0 \\ \hline P_\Delta B_\psi & 0 & A_\psi^\top P_\Delta + P_\Delta A_\psi \end{array} \right] \\ &\leq \lambda(\star)^\top \left[ \begin{array}{cccc|c} F & G_v & G_\xi & G_w & 0 \end{array} \right] \\ &+ \tau \left[ \begin{array}{cc|c} D_\psi^\top MD_\psi & 0 & D_\psi^\top MC_\psi \\ 0 & 0 & 0 \\ \hline C_\psi^\top MD_\psi & 0 & C_\psi^\top MC_\psi \end{array} \right], \end{aligned} \quad (19)$$

where  $X(P) := \begin{bmatrix} A^\top P + PA & PB_v & PB_\xi \\ B_v^\top P & 0 & 0 \\ B_\xi^\top P & 0 & 0 \end{bmatrix}$ . (The matrices in (19) are block partitioned to assist with readability.)

*Remark 1:* Conservatism of Proposition 1 arises from requiring a *single* storage function  $\tilde{V}(\cdot, \cdot)$  to ensure dissipativity *for all*  $\Delta$  satisfying a quadratic constraint. The benefit of this is the computational efficiency of considering feasibility of a single LMI to confirm dissipativity over the full uncertainty set.

When the uncertainties can be captured as the output of a system  $\Delta$  satisfying a *pointwise* quadratic constraint defined by  $(I, M)$ , the parameter  $P_\Delta$  accounting for the filter dynamics can be taken as zero, and condition (19) simplifies to

$$\begin{aligned} &\left[ \begin{array}{cccc|c} A^\top P + PA & PB_v & PB_\xi & PB_w \\ B_v^\top P & 0 & 0 & 0 \\ B_\xi^\top P & 0 & 0 & 0 \\ B_w^\top P & 0 & 0 & 0 \end{array} \right] \preceq \tau \tilde{M} + \\ &\left[ \begin{array}{cccc} X_{xx} & 0 & 0 & X_{xw} \\ 0 & 0 & 0 & 0 \\ 0 & 0 & 0 & 0 \\ X_{xw}^\top & 0 & 0 & X_{ww} \end{array} \right] + \lambda \left[ \begin{array}{c} F^\top \\ G_v^\top \\ G_\xi^\top \\ G_w^\top \end{array} \right] \left[ \begin{array}{c} F^\top \\ G_v^\top \\ G_\xi^\top \\ G_w^\top \end{array} \right]^\top \end{aligned} \quad (20)$$

where  $\tilde{M} := \begin{bmatrix} M & 0 \\ 0 & 0 \end{bmatrix}$ .

**Example 2: (Implicit neural network controller)**

Consider a general linear plant with dynamics

$$\begin{aligned} \dot{\mathbf{x}}_p(t) &= \mathbf{A}_p\mathbf{x}_p(t) + \mathbf{B}_u\mathbf{u}(t) + \mathbf{B}_w\mathbf{w}(t) \\ \mathbf{y}(t) &= \mathbf{C}_p\mathbf{x}_p(t) \end{aligned} \quad (21)$$

in feedback with a controller  $\pi_\theta$  modeled as the interconnection of an LTI system and activation

functions  $\phi$ :

$$\begin{aligned}\dot{\mathbf{x}}_k(t) &= A_k \mathbf{x}_k(t) + B_\xi \boldsymbol{\xi}(t) + B_y \mathbf{y}(t) \\ \mathbf{u}(t) &= C_u \mathbf{x}_k(t) + D_{u\xi} \boldsymbol{\xi}(t) + D_{uy} \mathbf{y}(t) \\ \mathbf{v}(t) &= C_v \mathbf{x}_k(t) + D_{v\xi} \boldsymbol{\xi}(t) + D_{vy} \mathbf{y}(t) \\ \boldsymbol{\xi} &= \phi(\mathbf{v}(t))\end{aligned}\quad (22)$$

with  $\theta := \begin{bmatrix} A_k & B_\xi & B_y \\ C_u & D_{u\xi} & D_{uy} \\ C_v & D_{v\xi} & D_{vy} \end{bmatrix}$  capturing the learnable parameters of  $\pi_\theta$ . In the terminology of [16], this controller is an ‘‘implicit’’ recurrent neural network, since  $D_{v\xi} \neq 0$  results in a fixed-point equation that implicitly defines the variable  $\boldsymbol{\xi}$ . This class of networks encompasses common architectures such as fully connected feedforward neural networks, convolutional layers, and max-pooling layers [16]. By incorporating feedback loops, implicit neural networks are able to achieve the performance of feedforward architectures with fewer parameters [28].

We assume the nonlinearity  $\phi$  is applied elementwise so that  $\phi(v) = [\phi_1(v_1) \cdots \phi_n(v_n)]^\top$  and each  $\phi_i$  is sector-bounded. Without loss of generality<sup>2</sup>, we take this sector to be  $[0, 1]$ , which is satisfied by common activation functions such as ReLU and tanh, so that

$$\begin{bmatrix} v \\ \boldsymbol{\xi} \end{bmatrix}^\top \begin{bmatrix} 0 & -\frac{1}{2}\Lambda \\ -\frac{1}{2}\Lambda & \Lambda \end{bmatrix} \begin{bmatrix} v \\ \boldsymbol{\xi} \end{bmatrix} \leq 0 \quad (23)$$

for any diagonal  $\Lambda \succ 0$ . The interconnection of plant (21) and controller  $\pi$  is described by

$$\begin{aligned}\dot{\mathbf{x}}(t) &= \mathbf{A}\mathbf{x}(t) + \mathbf{B}_w \mathbf{w}(t) + \mathbf{B}_\xi \boldsymbol{\xi}(t) \\ 0 &= \mathbf{C}\mathbf{x}(t) - \mathbf{v}(t) + \mathcal{D}\boldsymbol{\xi}(t) \\ \boldsymbol{\xi}(t) &= \phi(\mathbf{v}(t)),\end{aligned}\quad (24)$$

where  $\mathbf{x}(t) = \begin{bmatrix} \mathbf{x}_p(t) \\ \mathbf{x}_k(t) \end{bmatrix}$ , and

$$\begin{aligned}\mathbf{A} &= \begin{bmatrix} A_p + B_u D_{uy} C_p & B_u C_u \\ B_y C_p & A_k \end{bmatrix}, \mathbf{B}_w = \begin{bmatrix} B_w \\ 0 \end{bmatrix}, \\ \mathbf{B}_\xi &= \begin{bmatrix} B_u D_{u\xi} \\ B_\xi \end{bmatrix}, \mathbf{C} = [D_{vy} C_p \quad C_v], \mathcal{D} = D_{v\xi}.\end{aligned}$$

<sup>2</sup>If the sector is given by  $[\alpha, \beta] \neq [0, 1]$ , we may apply the loop transformation outlined in [29, Sec. II-D] to obtain an equivalent system sector bounded by  $[0, 1]$ .

Restrictions are placed on  $\mathcal{D}$  to ensure well-posedness of the interconnection, e.g., singular values of  $\mathcal{D}$  restricted to be less than one. Nonetheless, there are allowable values of  $\mathcal{D}$  that are singular; for these cases, the algebraic constraint can not be inverted to admit a standard ODE form for analysis.

Applying Proposition 1, an  $L_2$  gain from  $\mathbf{w}$  to  $\mathbf{y}$  of  $\gamma$  holds for the closed-loop system (24) if there exist  $P = P^\top \succ 0$ , diagonal  $\Lambda \succ 0$ , and scalar  $\lambda \geq 0$  for which the following LMI holds

$$\begin{aligned}& \begin{bmatrix} \mathbf{A}^\top P + P\mathbf{A} + \gamma^2 \begin{bmatrix} C_p^\top C_p & 0 \\ 0 & 0 \end{bmatrix} & P\mathbf{B}_w & 0 & P\mathbf{B}_\xi \\ & \mathbf{B}_w^\top P & -I & 0 & 0 \\ & 0 & 0 & 0 & 0 \\ & \mathbf{B}_\xi^\top P & 0 & 0 & 0 \end{bmatrix} \\ & \preceq \begin{bmatrix} 0 & 0 & 0 & 0 \\ 0 & 0 & 0 & 0 \\ 0 & 0 & 0 & -\frac{1}{2}\Lambda \\ 0 & 0 & -\frac{1}{2}\Lambda & \Lambda \end{bmatrix} + \lambda \begin{bmatrix} \mathbf{C}^\top \\ 0 \\ -I \\ \mathcal{D}^\top \end{bmatrix} [\mathbf{C} \quad 0 \quad -I \quad \mathcal{D}].\end{aligned}$$

This LMI is convex in  $P, \Lambda$ , and  $\lambda$ , so that feasibility can be checked numerically given parameters  $\theta$ . This provides a sufficient condition for a controller  $\pi_\theta$  to satisfy an  $L_2$  gain bound.

#### 1) Linear DAE without Uncertainty

The results presented thus far have provided *sufficient* conditions for dissipativity of uncertain DAE systems, where conservatism is introduced to reduce an associated computational burden. In the linear case with no uncertainty, this conservatism is eliminated, as summarized in the following proposition whose proof is in Appendix A.

*Proposition 2:* The linear DAE system (15), with  $\boldsymbol{\xi} = 0$ , is dissipative w.r.t. the quadratic supply rate (17) if and only if there exists  $\lambda \geq 0$  and a matrix  $P \succ 0$  such that

$$\begin{aligned}& \begin{bmatrix} \mathbf{A}^\top P + P\mathbf{A} & P\mathbf{B}_v & P\mathbf{B}_w \\ \mathbf{B}_v^\top P & 0 & 0 \\ \mathbf{B}_w^\top P & 0 & 0 \end{bmatrix} \preceq \\ & \begin{bmatrix} X_{xx} & 0 & X_{xw} \\ 0 & 0 & 0 \\ X_{xw}^\top & 0 & X_{ww} \end{bmatrix} + \lambda \begin{bmatrix} F^\top \\ G_v^\top \\ G_w^\top \end{bmatrix} [F \quad G_v \quad G_w].\end{aligned}\quad (25)$$

## V. CASE STUDY: POWER NETWORK WITH LINE FAILURES

We analyze the performance of a wide-area control policy for a power network in the event of a sin-

gle line failure, referred to as an  $N-1$  contingency [30]. Designing a separate control policy for each such contingency one-by-one is computationally burdensome. In fact, for large power networks it would be computationally intractable to perform this computation at the time-scale with which the operating conditions (and thus the dynamics of the system) change. Thus, it is advantageous to design a single controller and quickly verify its performance for a set of potential contingencies simultaneously. In this section, we use Proposition 1 for this task applied to the IEEE 39-bus power network [31].

#### A. Power Network & Line Failure Model

The dynamics at each of the 10 generators in the IEEE 39-bus network are modeled with the classical swing equations [32]:

$$\begin{aligned}\dot{\delta}_i(t) &= \Omega \omega_i(t) \\ \dot{\omega}_i(t) &= \frac{1}{2H_i} \left( p_{mi}(t) - D_i \omega_i(t) - \frac{E_i \mathbf{v}_{G_i}(t) \sin(\delta_i(t) - \theta_{G_i}(t))}{X_{di}} \right)\end{aligned}\quad (26)$$

where  $\tilde{\mathbf{E}}_i(t) = E_i e^{j\delta_i(t)}$  is the internal voltage,  $\tilde{\mathbf{v}}_{G_i} = \mathbf{v}_{G_i}(t) e^{j\theta_{G_i}(t)}$  is the bus voltage phasor,  $p_{mi}(t)$  is the mechanical input power, and  $H_i$ ,  $X_{di}$ , and  $D_i$  are the inertia, internal transient reactance and damping constants, all for the  $i^{\text{th}}$  generator. Linearization about a power flow solution gives

$$\begin{aligned}\frac{d}{dt} \begin{bmatrix} d\delta(t) \\ d\omega(t) \end{bmatrix} &= \bar{A} \begin{bmatrix} d\delta(t) \\ d\omega(t) \end{bmatrix} + \bar{B}_v \mathbf{v}(t) \\ &\quad + \begin{bmatrix} 0 \\ \mathbf{w}(t) + \mathbf{u}(t) \end{bmatrix},\end{aligned}\quad (27)$$

where  $\mathbf{u}$  and  $\mathbf{w}$  represent vectors of control and disturbance signals, respectively, and  $d\delta$  and  $d\omega$  denote vectors of the deviation of  $\delta$  and  $\omega$  from their operating points  $\delta_0$  and  $\omega_0 = 0$ . The generator dynamics are coupled through the network via the power flow equations:

$$\left( \begin{bmatrix} Y_{11} & Y_{12} \\ Y_{21} & Y_{22} \end{bmatrix} + \begin{bmatrix} Y_d & 0 \\ 0 & Y_L \end{bmatrix} \right) \begin{bmatrix} \tilde{\mathbf{v}}_G(t) \\ \tilde{\mathbf{v}}_L(t) \end{bmatrix} = \begin{bmatrix} Y_d \tilde{\mathbf{E}}(t) \\ 0 \end{bmatrix}$$

where  $\tilde{\mathbf{v}}_{L_i}(t) = \mathbf{v}_{L_i}(t) e^{j\theta_{L_i}(t)}$  is the voltage phasor at load bus  $i$ ,  $\begin{bmatrix} Y_{11} & Y_{12} \\ Y_{21} & Y_{22} \end{bmatrix}$  is the network admittance matrix,  $Y_d$  is a diagonal matrix whose entries are the inverses of the generator internal

transient reactances,  $\frac{1}{X_{di}}$ , and  $Y_L$  is a diagonal matrix whose entries are the constant impedance models of loads in the network. Linearizing this complex-valued equation about the power flow solution and separating real and imaginary components gives the linear, real-valued algebraic constraint

$$0 = \bar{F} \begin{bmatrix} d\delta(t) \\ d\omega(t) \end{bmatrix} + G \mathbf{v}(t), \quad (28)$$

where

$$\mathbf{v}(t) := \begin{bmatrix} d\mathbf{v}_G(t)^\top & d\boldsymbol{\theta}_G(t)^\top & d\mathbf{v}_L(t)^\top & d\boldsymbol{\theta}_L(t)^\top \end{bmatrix}^\top$$

is the deviation of magnitudes ( $\mathbf{v}_G, \mathbf{v}_L$ ) and angles ( $\boldsymbol{\theta}_G, \boldsymbol{\theta}_L$ ) of the voltages at generator and load buses from their operating points, respectively. (Appendix C provides expressions for  $\bar{A}, \bar{B}_v, \bar{F}$ , and  $G$ .) We evaluate performance with the output

$$\mathbf{y}(t) = \begin{bmatrix} 0 & I \end{bmatrix} \begin{bmatrix} d\delta(t) \\ d\omega(t) \end{bmatrix} =: \bar{C} \begin{bmatrix} d\delta(t) \\ d\omega(t) \end{bmatrix}. \quad (29)$$

For controller design, we assume access to *relative* angle measurements, e.g.  $d\delta_1 - d\delta_2$  and absolute angular velocity measurements, e.g.  $d\omega_1$ . A linear, static controller will then take the form [33]

$$\mathbf{u}(t) = K \mathbf{x}(t), \quad (30)$$

where  $\mathbf{x}(t) = Q \begin{bmatrix} d\delta(t) \\ d\omega(t) \end{bmatrix}$  is a reduced state vector and  $Q$  is a matrix whose columns form an orthonormal basis for the null space of  $\begin{bmatrix} \mathbb{1}^\top & 0 \end{bmatrix}$ . The corresponding reduced dynamics are

$$\begin{aligned}\dot{\mathbf{x}}(t) &= A \mathbf{x}(t) + B_v \mathbf{v}(t) + B_w (\mathbf{w}(t) + \mathbf{u}(t)) \\ 0 &= F \mathbf{x}(t) + G \mathbf{v}(t) \\ \mathbf{y} &= C \mathbf{x}(t),\end{aligned}\quad (31)$$

where  $A = Q^\top \bar{A} Q$ ,  $B_v = Q^\top \bar{B}_v$ ,  $B_w = Q^\top \begin{bmatrix} 0 & I \end{bmatrix}^\top$ ,  $F = \bar{F} Q$  and  $C = \bar{C} Q$ . The input-output behavior of (31) is equivalent to that of the original system (27)-(29), because (i) the DAE (27)-(28) is invariant to uniform shifts in angles, i.e.,

$$\bar{A} \begin{bmatrix} \mathbb{1} \\ 0 \end{bmatrix} = 0, \quad \bar{F} \begin{bmatrix} \mathbb{1} \\ 0 \end{bmatrix} + G \begin{bmatrix} 0 \\ \mathbb{1} \\ 0 \\ \mathbb{1} \end{bmatrix} = 0, \quad (32)$$

and (ii) the mode corresponding to these uniform angle shifts is unobservable from output (29).

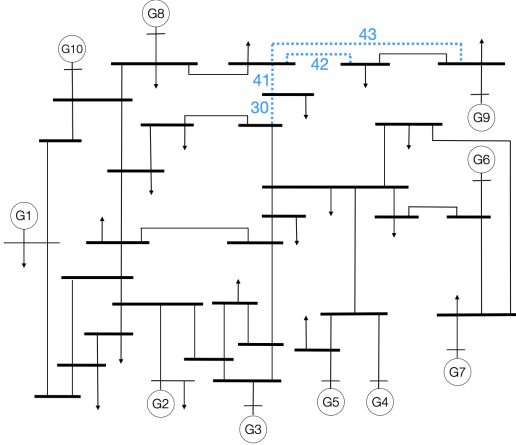


Fig. 2. IEEE 39-Bus Network with potential line failures indicated with dashed blue lines.

### 1) Line Failure Model & Controller Design

We restrict our attention to line failures that do not disconnect the underlying graph structure; this corresponds to the vast majority of lines in a typical network [34]. For instance, we do not consider line failures that result in the disconnection of a generator. In this setting, the dynamics of the perturbed system remain approximately linear.

We consider four line failures of interest: lines 30, 41, 42, and 43 (see Figure 2). We design a controller (30) to place all closed-loop eigenvalues in the half plane  $\{z; \Re(z) < -0.5\}$  for the dynamics resulting from line 43 failing. The closed-loop dynamics in this case are approximately

$$\dot{\mathbf{x}}(t) = A_{cl}\mathbf{x}(t) + B_v\mathbf{v}(t) + B_w\mathbf{w}(t) \quad (33a)$$

$$0 = F\mathbf{x}(t) + (G + \Delta G_{43})\mathbf{v}(t) \quad (33b)$$

$$\mathbf{y}(t) = C\mathbf{x}(t), \quad (33c)$$

where  $A_{cl} := (A + B_uK)$ , and the change to the closed-loop dynamics due to the removal of line 43 is approximated by the additive perturbation  $\Delta G_{43}$ .

Our objective is to verify  $H_\infty$  performance of the system in feedback with this wide-area controller for any of the line failures of interest. Rather than checking each line failure one-by-one, we prioritize computationally tractability by constructing a (conservative) uncertainty set containing each contingency, and verifying dissipativity ( $L_2$ -gain bound) over this uncertainty set through one LMI using

Proposition 1.

To create this uncertainty set, we approximate the change in the closed-loop dynamics due to the failure of line  $i$  as an additive perturbation  $\Delta G_i$  to  $G$ . We compute the differences  $\Delta G_i - \Delta G_{43}$  for  $i = 30, 41, 42$ . The magnitudes of the singular values of these differences drop off rapidly, and thus we approximate each by a “structured” [35] rank three matrix, where “structure” corresponds to preserving the physical property (32):  $\Delta G_{41} - \Delta G_{43} = H_1 J_1^\top$ ,  $\Delta G_{42} - \Delta G_{43} = H_2 J_2^\top$ ,  $\Delta G_{30} - \Delta G_{43} = H_3 J_3^\top$ , with  $H_i, J_i \in \mathbb{R}^{78 \times 3}$ . Then,

$$0 = F\mathbf{x} + (G + \Delta G_{43})\mathbf{v} + \sum_{i=1}^3 \frac{1-\theta_i}{2} H_i J_i^\top \mathbf{v}, \quad (34)$$

$\theta_i \in [-1, 1]$ , covers the algebraic constraint corresponding to each of the four line failures of interest, e.g.,  $\theta_1 = \theta_2 = \theta_3 = 1$  and  $\theta_1 = -1, \theta_2 = \theta_3 = 1$  correspond to the removal of line 43 and 41, respectively. This uncertainty is incorporated as

$$\begin{aligned} \dot{\mathbf{x}}(t) &= A_{cl}\mathbf{x}(t) + B_v\mathbf{v}(t) + B_w\mathbf{w}(t), \\ 0 &= F\mathbf{x}(t) + G_v\mathbf{v}(t) + G_\xi\xi(t), \\ \mathbf{y}(t) &= C\mathbf{x}(t), \end{aligned} \quad (35)$$

where

$$\begin{aligned} G_\xi &= [H_1 \ H_2 \ H_3], \\ G_v &= G + \Delta G_{43} + \frac{1}{2} (H_1 J_1^\top + H_2 J_2^\top + H_3 J_3^\top) \end{aligned} \quad (36)$$

and  $\xi(t) = [\xi_1(t)^\top \ \xi_2(t)^\top \ \xi_3(t)^\top]^\top$  is the output of some  $\Delta$  satisfying the pointwise quadratic constraints

$$\begin{bmatrix} \xi_i \\ v \end{bmatrix}^\top \begin{bmatrix} X_i & \frac{-1}{2} Y_i J_i^\top \\ \frac{-1}{2} J_i Y_i^\top & \frac{-1}{4} J_i X_i J_i^\top \end{bmatrix} \begin{bmatrix} \xi_i \\ v \end{bmatrix} \leq 0 \quad (37)$$

for any  $X_i = X_i^\top \succeq 0$  and  $Y_i = -Y_i^\top$  [4].

*Remark 2:* This uncertainty set could be equivalently characterized by a polytopic set, as in [13, Sec. 3]. Characterization (37) results in a lower dimensional LMI condition and allows us to incorporate the uncertainty set parameters  $X_i, Y_i$  as additional design variables for more flexibility.

### B. $H_\infty$ Norm Bound over a set of Line Failures

We compute a bound on the  $L_2$  gain from  $\mathbf{w}$  to  $\mathbf{y}$  of (35)-(36) with  $\Delta$  satisfying (37) using Proposition 1. We formulate the corresponding convex



optimization problem

$$\begin{aligned}
& \min_{P, \lambda, X_1, Y_1, X_2, Y_2, \gamma^2} \gamma^2 \\
& \text{s.t. } P \succ 0, X_i = X_i^\top \succeq 0, Y_i = -Y_i^\top, \lambda \geq 0, \\
& \begin{bmatrix} A_{\text{cl}}^\top P + P A_{\text{cl}} + C^\top C & P B_v & 0 & P B_w \\ B_v^\top P & 0 & 0 & 0 \\ 0 & 0 & 0 & 0 \\ B_w^\top P & 0 & 0 & -\gamma^2 I \end{bmatrix} \\
& \preceq \lambda \begin{bmatrix} F^\top \\ G_v^\top \\ G_\xi^\top \\ 0 \end{bmatrix} \begin{bmatrix} F & G_v & G_\xi & 0 \end{bmatrix} + \\
& \begin{bmatrix} 0 & 0 & 0 & 0 \\ 0 & \frac{-1}{4} \sum_{i=1}^3 (J_i X_i J_i^\top) & W & 0 \\ 0 & W^\top & X & 0 \\ 0 & 0 & 0 & 0 \end{bmatrix} \quad (38)
\end{aligned}$$

where  $W := \frac{-1}{2} [J_1 Y_1^\top \ J_2 Y_2^\top \ J_3 Y_3^\top]$  and  $X$  is the block diagonal matrix of  $\{X_1, X_2, X_3\}$ . We solve (38) numerically in MATLAB using CVX [36] with the SeDuMi solver [25] resulting in an  $L_2$  gain bound of  $\gamma = 2.31$  over the uncertainty set. To evaluate conservatism, we compute the  $L_2$  gain corresponding to each of the four line removals:

Line removed	30	41	42	43
Closed-loop $H_\infty$ -norm	2.215	2.222	2.219	2.217

We compute  $L_2$  gains over the full uncertainty set via a grid search - the maximum value obtained is 2.2719, occurring at  $\theta_1 = 0.1, \theta_2 = 0, \theta_3 = 0$  in (34); note that this point does not correspond to a physical line removal.

We analyze the amount of conservatism introduced by our methodology. Our bound  $\gamma = 2.31$  is 3.98% over the true maximal  $L_2$  gain over the four line removals of interest and 1.68% over true bound for the full uncertainty set. Thus, for this case study, neither the choice of a larger uncertainty set nor the restriction to a single storage function cause much conservatism. An added benefit of this approach is the implicit incorporation of robustness.

We remark on how this methodology compares to an alternate approach of modeling the power network equations as an ODE, rather than a DAE. An advantage of the DAE framework is that it

allows for line failures to be modeled as uncertain low rank perturbations to the matrix  $G_v$ . If we instead utilized the equivalent power network model

$$\dot{x}(t) = (A_{\text{cl}} - B_v G_v^{-1} F)x(t) + B_w w(t), \quad (39)$$

perturbations to  $G_v$  would need to be inverted to obtain perturbations on the matrix  $(A_{\text{cl}} - B_v G_v^{-1} F)$ , eliminating the structure that allows for simple characterization of the uncertainty set utilized.

More generally, whenever the algebraic condition (1b) of a DAE is invertible, the dynamics could be equivalently represented by an ODE. This approach will not apply to general DAE systems, whose algebraic conditions may not be invertible. Even with invertibility, the DAE form might be advantageous in (i) preserving structure captured by the algebraic constraint or (ii) avoiding inversion of a poorly conditioned matrix.

## VI. CONCLUSION

A general framework for dissipativity analysis of DAE systems with uncertainties described by IQCs was provided. Numerical methods for verifying sufficient conditions for dissipativity of these systems in the case of polynomial or linear dynamics were illustrated. Analysis of the IEEE 39-bus power system subject to line failures provided a case study that highlighted the amount of conservatism introduced by sufficient conditions could be quite minimal; quantifying or minimizing this conservatism could be examined in future work. Further analysis of this case study is also the subject of ongoing work, e.g., efficient methods to group together sets of line failures to characterize by uncertainty sets is currently being investigated [37].

## REFERENCES

- [1] J. C. Willems, "Dissipative dynamical systems part I: General theory," *Archive for rational mechanics and analysis*, vol. 45, no. 5, pp. 321–351, 1972.
- [2] R. Lozano, B. Brogliato, O. Egeland, and B. Maschke, *Dissipative systems analysis and control: theory and applications*. Springer Science & Business Media, 2013.
- [3] B. Hu, M. J. Lacerda, and P. Seiler, "Robustness analysis of uncertain discrete-time systems with dissipation inequalities and integral quadratic constraints," *International Journal of Robust and Nonlinear Control*, vol. 27, no. 11, pp. 1940–1962, 2017.

- [4] A. Megretski and A. Rantzer, "System analysis via integral quadratic constraints," *IEEE transactions on automatic control*, vol. 42, no. 6, pp. 819–830, 1997.
- [5] S. Xie, L. Xie, and C. E. De Souza, "Robust dissipative control for linear systems with dissipative uncertainty," *International Journal of Control*, vol. 70, no. 2, pp. 169–191, 1998.
- [6] A. Kumar and P. Daoutidis, *Control of nonlinear differential algebraic equation systems with applications to chemical processes*, vol. 397. CRC Press, 1999.
- [7] U. M. Ascher and L. R. Petzold, *Computer methods for ordinary differential equations and differential-algebraic equations*, vol. 61. Siam, 1998.
- [8] E. Yip and R. Sincovec, "Solvability, controllability, and observability of continuous descriptor systems," *IEEE transactions on Automatic Control*, vol. 26, no. 3, pp. 702–707, 1981.
- [9] Y. Feng and M. Yagoubi, *Robust control of linear descriptor systems*. Springer, 2017.
- [10] M. Darouach and M. Boutayeb, "Design of observers for descriptor systems," *IEEE transactions on Automatic Control*, vol. 40, no. 7, pp. 1323–1327, 1995.
- [11] D. Chu and R. C. Tan, "Algebraic characterizations for positive realness of descriptor systems," *SIAM Journal on Matrix Analysis and Applications*, vol. 30, no. 1, pp. 197–222, 2008.
- [12] P. Liu, Q. Zhang, X. Yang, and L. Yang, "Passivity and optimal control of descriptor biological complex systems," *IEEE Transactions on Automatic Control*, vol. 53, no. Special Issue, pp. 122–125, 2008.
- [13] E. Uezato and M. Ikeda, "Strict LMI conditions for stability, robust stabilization, and  $h_\infty$  control of descriptor systems," in *Proceedings of the 38th IEEE Conference on Decision and Control (Cat. No. 99CH36304)*, vol. 4, pp. 4092–4097, IEEE, 1999.
- [14] F. E. Udawadia and P. Phohomsiri, "Explicit equations of motion for constrained mechanical systems with singular mass matrices and applications to multi-body dynamics," *Proceedings of the Royal Society A: Mathematical, Physical and Engineering Sciences*, vol. 462, no. 2071, pp. 2097–2117, 2006.
- [15] H. Choi, P. J. Seiler, and S. V. Dhople, "Propagating uncertainty in power-system dae models with semidefinite programming," *IEEE Transactions on Power Systems*, vol. 32, no. 4, pp. 3146–3156, 2017.
- [16] L. E. Ghaoui, F. Gu, B. Travacca, A. Askari, and A. Y. Tsai, "Implicit deep learning," 2020.
- [17] F. Dorfler and F. Bullo, "Kron reduction of graphs with applications to electrical networks," *IEEE Transactions on Circuits and Systems I: Regular Papers*, vol. 60, no. 1, pp. 150–163, 2012.
- [18] J.-Y. Lin and Z.-H. Yang, "Existence and uniqueness of solutions for non-linear singular (descriptor) systems," *International journal of systems science*, vol. 19, no. 11, pp. 2179–2184, 1988.
- [19] S. Reich, "On an existence and uniqueness theory for non-linear differential-algebraic equations," *Circuits, Systems and Signal Processing*, vol. 10, pp. 343–359, 1991.
- [20] P. J. Rabier and W. C. Rheinboldt, "A geometric treatment of implicit differential-algebraic equations," *Journal of Differential Equations*, vol. 109, no. 1, pp. 110–146, 1994.
- [21] W. C. Rheinboldt, "Differential-algebraic systems as differential equations on manifolds," *Mathematics of computation*, vol. 43, no. 168, pp. 473–482, 1984.
- [22] S. L. Campbell and E. Griepentrog, "Solvability of general differential algebraic equations," *SIAM Journal on Scientific Computing*, vol. 16, no. 2, pp. 257–270, 1995.
- [23] P. Seiler, A. Packard, and G. J. Balas, "A dissipation inequality formulation for stability analysis with integral quadratic constraints," in *49th IEEE Conference on Decision and Control (CDC)*, pp. 2304–2309, IEEE, 2010.
- [24] S. Prajna, A. Papachristodoulou, and P. A. Parrilo, "Introducing sostoools: A general purpose sum of squares programming solver," in *Proceedings of the 41st IEEE Conference on Decision and Control, 2002.*, vol. 1, pp. 741–746, IEEE, 2002.
- [25] J. F. Sturm, "Using SeDuMi 1.02, a MATLAB toolbox for optimization over symmetric cones," *Optimization methods and software*, vol. 11, no. 1-4, pp. 625–653, 1999.
- [26] J. Buch, S.-C. Liao, and P. Seiler, "Robust control barrier functions with sector-bounded uncertainties," *IEEE Control Systems Letters*, vol. 6, pp. 1994–1999, 2021.
- [27] H. Hindi and S. Boyd, "Analysis of linear systems with saturation using convex optimization," in *Proceedings of the 37th IEEE conference on decision and control (Cat. No. 98CH36171)*, vol. 1, pp. 903–908, IEEE, 1998.
- [28] S. Bai, J. Z. Kolter, and V. Koltun, "Deep equilibrium models," 2019.
- [29] N. Junnarkar, H. Yin, F. Gu, M. Arcak, and P. Seiler, "Synthesis of stabilizing recurrent equilibrium network controllers," in *2022 IEEE 61st Conference on Decision and Control (CDC)*, pp. 7449–7454, IEEE, 2022.
- [30] N. Xue, X. Wu, S. Gumussoy, U. Muenz, A. Mesanovic, C. Heyde, Z. Dong, G. Bharati, S. Chakraborty, L. Cockcroft, *et al.*, "Dynamic security optimization for N-1 secure operation of hawaii island system with 100% inverter-based resources," *IEEE Transactions on Smart Grid*, vol. 13, no. 5, pp. 4009–4021, 2021.
- [31] T. Athay, R. Podmore, and S. Virmani, "A practical method for the direct analysis of transient stability," *IEEE Transactions on Power Apparatus and Systems*, no. 2, pp. 573–584, 1979.
- [32] J. H. Chow and J. J. Sanchez-Gasca, *Power system modeling, computation, and control*. John Wiley & Sons, 2020.
- [33] X. Wu, F. Dörfler, and M. R. Jovanović, "Input-output analysis and decentralized optimal control of inter-area oscillations in power systems," *IEEE Transactions on Power Systems*, vol. 31, no. 3, pp. 2434–2444, 2015.
- [34] S. A. J. Taft, "Connectivity, centrality, and bottleneckedness: On graph theoretic methods for power systems," 2020.
- [35] M. T. Chu, R. E. Funderlic, and R. J. Plemmons, "Structured low rank approximation," *Linear algebra and its applications*, vol. 366, pp. 157–172, 2003.
- [36] M. Grant and S. Boyd, "CVX: MATLAB software for disciplined convex programming, version 2.1." [url=http://cvxr.com/cvx](http://cvxr.com/cvx), Mar. 2014.
- [37] N. Junnarkar, E. Jensen, X. Wu, S. Gumussoy, and M. Arcak, "Grouping of  $n - 1$  contingencies for controller synthesis: A study for power line failures," *Under Review, ArXiv preprint 2404.07415*, 2024.

[38] S. Boyd, S. P. Boyd, and L. Vandenberghe, *Convex optimization*. Cambridge university press, 2004.

## APPENDIX

### A. Proof of Proposition 2

By the lossless S-procedure (see, e.g., [38]), the existence of  $\lambda \geq 0$  satisfying (25) is equivalent to nonpositivity of

$$\begin{bmatrix} x \\ v \\ w \end{bmatrix}^\top \begin{bmatrix} F^\top \\ G_v^\top \\ G_w^\top \end{bmatrix} [F \ G_v \ G_w] \begin{bmatrix} x \\ v \\ w \end{bmatrix} \quad (40)$$

implying

$$\begin{bmatrix} x \\ v \\ w \end{bmatrix}^\top \left( \begin{bmatrix} A^\top P + PA & PB_v & PB_w \\ B_v^\top P & 0 & 0 \\ B_w^\top P & 0 & 0 \end{bmatrix} - \begin{bmatrix} X_{xx} & 0 & X_{xw} \\ 0 & 0 & 0 \\ X_{xw}^\top & 0 & X_{ww} \end{bmatrix} \right) \begin{bmatrix} x \\ v \\ w \end{bmatrix} \leq 0. \quad (41)$$

Since  $V(\cdot)$  is continuously differentiable, dissipativity (Definition 1) with  $\xi = 0$  can be confirmed through the differential characterization that:

$$0 = g(x, v, w, 0) \Rightarrow \nabla V(x)^\top f(x, v, w, 0) \leq 0$$

for all  $x, v, w$ . Nonpositivity of (40) is equivalent to  $0 = g(x, v, w, 0)$  for linear  $g$  of the form (15b), and condition  $\nabla V(x)^\top f(x, v, w, 0) \leq 0$  reduces to (41) for linear  $f$  of form (15a) and quadratic  $V$ . ■

### B. Proof of Theorem 1:

Assume (19) holds, and left and right the inequality by  $[x^\top \ v^\top \ \xi^\top \ w^\top \ \psi^\top]$  and its transpose to arrive at the following condition, which is equivalent to (8) in this linear setting:

$$\begin{aligned} & x^\top P(Ax + B_v v + B_w w + B_\xi \xi) + (\star)^\top P x + \\ & \psi^\top P_\Delta \left( A_\psi^\top \psi(t) + B_\psi \begin{bmatrix} x(t) \\ v(t) \\ \xi(t) \end{bmatrix} \right) + (\star)^\top P_\Delta \psi(t) \\ & \leq \begin{bmatrix} x \\ w \end{bmatrix}^\top \begin{bmatrix} X_{xx} & X_{xw} \\ X_{xw}^\top & X_{ww} \end{bmatrix} \begin{bmatrix} x \\ w \end{bmatrix} \\ & + \lambda \begin{bmatrix} x \\ v \\ \xi \\ w \end{bmatrix}^\top \begin{bmatrix} F^\top \\ G_v^\top \\ G_\xi^\top \\ G_w^\top \end{bmatrix} [F \ G_v \ G_\xi \ G_w] \begin{bmatrix} x \\ v \\ \xi \\ w \end{bmatrix} \\ & + \tau \left( C_\psi \psi + D_\psi \begin{bmatrix} x \\ v \\ \xi \end{bmatrix} \right)^\top M \left( C_\psi \psi + D_\psi \begin{bmatrix} x \\ v \\ \xi \end{bmatrix} \right), \end{aligned}$$

where each of term  $(\star)$  may be inferred by symmetry. The result then follows from Theorem 1. ■

### C. Power Network Model Parameters:

The ODE parameters are given by

$$\begin{aligned} \bar{A} &= \begin{bmatrix} 0_{n_g \times n_g} & \Omega \cdot I_{n_g} \\ \text{diag}\left(\frac{-E \circ V_G \circ \cos(\delta - \theta_G)}{2H \circ X_d}\right) & \text{diag}\left(\frac{-D}{2H}\right) \end{bmatrix} \\ \bar{B} &= \begin{bmatrix} 0_{n_g \times n_g} & 0_{n_g \times n_g} & 0_{n_g \times n_l} & 0_{n_g \times n_l} \\ \bar{B}_{21} & \bar{B}_{22} & 0_{n_g \times n_l} & 0_{n_g \times n_l} \end{bmatrix}, \end{aligned}$$

where  $\bar{B}_{21} = \text{diag}\left(\frac{-E \circ \sin(\delta - \theta_G)}{2H \circ X_d}\right)$ , and  $\bar{B}_{22} = \text{diag}\left(\frac{E \circ V_G \circ \cos(\delta - \theta_G)}{2H \circ X_d}\right)$ . To define  $\bar{F}$  and  $G$ , we decompose the following matrices into real and imaginary parts:

$$\begin{aligned} Y_d &= Y_{\text{re}}^d + iY_{\text{im}}^d, \\ Y^G &= \begin{bmatrix} Y_{11} + Y_d \\ Y_{21} \end{bmatrix} = Y_{\text{re}}^G + iY_{\text{im}}^G, \\ Y^L &= \begin{bmatrix} Y_{12} \\ Y_{22} + Y_L \end{bmatrix} = Y_{\text{re}}^L + iY_{\text{im}}^L. \end{aligned}$$

With this notation,

$$\begin{aligned} \bar{F} &= \begin{bmatrix} Y_{\text{im}}^d \cdot \text{diag}(E \circ \cos(\delta)) & 0_{n_g \times n_g} \\ 0_{n_l \times n_g} & 0_{n_l \times n_g} \\ Y_{\text{im}}^d \cdot \text{diag}(E \circ \sin(\delta)) & 0_{n_g \times n_g} \\ 0_{n_l \times n_g} & 0_{n_l \times n_g} \end{bmatrix} \\ G &= [G_{V_G} \ G_{\theta_G} \ G_{V_L} \ G_{\theta_L}], \end{aligned}$$

where

$$\begin{aligned} G_{V_G} &= \begin{bmatrix} Y_{\text{re}}^G \cdot \text{diag}(\cos \theta_G) - Y_{\text{im}}^G \cdot \text{diag}(\sin \theta_G) \\ Y_{\text{re}}^G \cdot \text{diag}(\sin \theta_G) + Y_{\text{im}}^G \cdot \text{diag}(\cos \theta_G) \end{bmatrix} \\ G_{\theta_G} &= \begin{bmatrix} -Y_{\text{re}}^G \cdot \text{diag}(V_G \circ \sin \theta_G) - Y_{\text{im}}^G \cdot \text{diag}(V_G \circ \cos \theta_G) \\ Y_{\text{re}}^G \cdot \text{diag}(V_G \circ \cos \theta_G) - Y_{\text{im}}^G \cdot \text{diag}(V_G \circ \sin \theta_G) \end{bmatrix} \\ G_{V_L} &= \begin{bmatrix} Y_{\text{re}}^L \cdot \text{diag}(\cos \theta_L) - Y_{\text{im}}^L \cdot \text{diag}(\sin \theta_L) \\ Y_{\text{re}}^L \cdot \text{diag}(\sin \theta_L) + Y_{\text{im}}^L \cdot \text{diag}(\cos \theta_L) \end{bmatrix} \\ G_{\theta_L} &= \begin{bmatrix} -Y_{\text{re}}^L \cdot \text{diag}(V_L \circ \sin \theta_L) - Y_{\text{im}}^L \cdot \text{diag}(V_L \circ \cos \theta_L) \\ Y_{\text{re}}^L \cdot \text{diag}(V_L \circ \cos \theta_L) - Y_{\text{im}}^L \cdot \text{diag}(V_L \circ \sin \theta_L) \end{bmatrix} \end{aligned}$$